Nuclear Instruments and Methods in Physics Research A300 (1991) 164–178
North-Holland

Study of the neutron field from a hadronic cascade in iron: verification of a Monte Carlo calculational model by comparison with measured data

J.M. Zazula [1] and K. Tesch

Deutsches Elektronen-Synchrotron DESY, Notkestrasse 85, W-2000 Hamburg 52, Germany

Received 21 May 1990 and in revised form 31 August 1990

The Monte Carlo code FLUNEV, an extension of the hadronic shower code FLUKA for production and transport of neutrons below 50 MeV, is modified by reduction both of the total energy carried by intranuclear cascade particles and of the excitation energy preceding the evaporation step in inelastic hadron–nucleus collisions, following phenomenological suggestions given by Alsmiller and Alsmiller (Nucl. Instr. and Meth. A278 (1989) 713, ref. [11]) and by Barashenkov et al. (Dubna report JINR/E2-89-437 (1989), ref. [10]). The modified version of our code is verified by comparison with experimental neutron distributions around thin iron targets and thick iron absorbers irradiated by high energy protons, and with earlier calculations of neutron fields. Good agreement is achieved in most cases.

1. Introduction

Estimation of fluences, energy distributions and absorbed doses due to secondary neutrons produced by high energy hadronic beams incident on various absorbers is an extensively studied experimental and theoretical problem of many practical implications [1–6]. Neutrons are a copious and one of the most penetrating components of the hadronic cascades, with energies covering many orders of magnitude, from the primary beam energy down to thermal energy. They are produced in high energy hadronic interactions, in photoproduction reactions occurring in electromagnetic showers produced by π^0 decays, in the intranuclear cascade process, in deexcitation of the residual nuclei after inelastic collisions and in low energy multiplying reactions like (n, 2n) or fission. Neutrons or their secondaries significantly contribute to absorbed doses and radiation damage in accelerator parts and to dose equivalents in an accelerator environment. Their detection has an important application for compensation between the hadronic and the electromagnetic signals in calorimeters constructed or designed for high energy colliders.

Experimental works concerning neutron field measurements at high energy proton accelerators and earlier theoretical papers have been reviewed by Tesch and Dinter [1] and by Thomas and Stevenson [2]. An especially important case is the proton beam incident on a thick iron absorber, since iron is used at proton accelerators as one of the basic materials for construction of magnets, beam dumps, radiation shielding and some types of calorimeters. Further references for this case can be found in the recent CERN report [3] providing the results of neutron fluence measurements using the activation detector technique at a calorimeter-like structure irradiated by 200 GeV/c protons. In the present article these results will be compared with our calculational model verified in course of the current work.

The most advanced method for estimating secondary neutron production from hadronic cascades is using Monte Carlo (MC) computer codes involving theoretical models of high energy hadron–nucleon and hadron–nucleus collisions and the simulation of particle transport and energy losses in realistic geometries. However, the common deficiency of these particles shower codes, when applied to calculations of the neutron field, is the use of a cut-off energy for secondary particle transport between 20 and 50 MeV. The main reason for this limitation is that low energy nuclear reactions have cross sections too complicated for parametrization within one generalized model, and, moreover, incorporation of the slow particle random walk is considered as leading to prohibitively long calculation times. Therefore, in some of the sophisticated code systems (e.g. CALOR [25] or HERMES [26]) developed for the purpose of hadronic calorimetry studies, the high energy particle transport code HETC [20] has externally been coupled to the low energy neutron

[1] On leave of absence from the Institute of Nuclear Physics, Krakow, Poland.

and gamma ray transport code MORSE [23], supported by a special data library containing multigroup neutron and photon cross sections.

Another important cascade program widely used for solution of practical problems is the FLUKA code [21] originated by the Leipzig theoretical group and extensively developed at CERN. Superiority of FLUKA over other codes applicable at high energy accelerators was achieved by implementation of the advanced event generator EVENTQ [7] based on the exclusive multichain fragmentation (dual parton) model. The deficiency of this code when compared with the somewhat complementary by considerably slower HETC is the rather crude treatment of the intranuclear cascade and deexcitation phenomena, based on semi-empirical parametrizations instead of detailed step-by-step simulation of these processes. The basic difficulty when trying to couple FLUKA to low energy neutron transport codes is that the complete process of secondary emission during deexcitation (the succeeding particle energies and directions) is not sampled by the original model of this code.

To overcome this problem, in some extensions of FLUKA [27,5] these neutrons were additionally generated from the Maxwell energy distribution according to the statistical model of nuclear evaporation, assuming re-equilibrium of energy between nucleons between successive emissions, until the excitation energy is exhausted. In our previous work [4] we developed the enhanced version of FLUKA, the FLUNEV code, linking together into one program the original high energy part, the MC evaporation module EVAP-5 taken from HETC/KFA [15], and a low energy neutron transport module. The latter is based on FLUKA geometry, a neutron collision package taken from MORSE, and a part of the HILO [30] multigroup cross section data from 50 MeV down to thermal neutron energy. In the referred paper we presented the radiation protection quantities of interest (dose equivalent and absorbed dose in tissue, particle currents emerging from a shield, mean quality factors) as obtained from FLUNEV for lateral ordinary concrete and heavy concrete shielding of proton accelerators.

Meanwhile, severe doubts have arised (see discussion and papers referred in the next section) if the total energy of intranuclear cascade nucleons, E_{inc}, and the nuclear excitation energy, E_{ex}, can be correctly determined by the inelastic collision module of FLUKA code (the EVENTQ event generator) preceding deexcitation. Note also that some physical processes becoming important at present day colliders, like photo- and electroproduction of hadrons, fragmentation of light nuclei or emission of secondaries from preequilibrium nuclear states have still not been accurately accounted for in hadronic cascade codes [8]. It became apparent to us that the direct verification of the models implemented into high energy transport codes can be done in reliable manner only by comparison with experiments performed with thin targets, which is the subject of section 2 of this paper. Unfortunately, the experimental data on the yields of secondary neutrons and on their angular and energy distributions are still far from complete.

Nevertheless, existing empirical material forced us to make some revisions in the determination of the E_{inc} and E_{ex} energies within our code (see section 2.1). We made these modifications following the suggestions contained in the papers of F.S. and R.G. Alsmiller [11] and of Barashenkov et al. [10]. Comparison with measurements and earlier calculations for thick iron targets is the subject of section 3. Particularly, in section 3.1 we examine the consequences of our modifications for thick target results and we argue that they could not significantly affect our previous results for the lateral concrete shielding. Additionally, we present a check of the low energy neutron transport module in FLUNEV for the case of a purely neutronic beam incident on iron. An important comparison with the recent iron absorber experiment performed at CERN [3] is the subject of the last section 3.2, providing also the plots of neutron spectra for various positions in the iron absorber which could be of practical interest for designing accelerator components, shielding and detectors.

2. Changes in inelastic interaction model and comparison with thin target experiments and calculations

2.1. Energy of intranuclear cascade, excitation energy and production of residual nuclei

In addition to the direct neutron production in hadron–nucleon interactions, the other phases of inelastic hadron–nucleus collisions contributing to emission of secondary neutrons are the intranuclear cascade and deexcitation. The common feature of the intranuclear cascade energy E_{inc} and of the excitation energy E_{ex}, as they appear in MC shower codes, is that they both represent model-dependent parameters that cannot be directly measured, but, instead, can be evaluated from other experimentally determined quantities (e.g. secondary multiplicities or differential cross sections) assuming a certain model (e.g. statistical theory of evaporation). Other input parameters used for the EVAP module in the FLUNEV code are the atomic number Z and mass number A of the residual nucleus left after the high energy particle emission and after the intranuclear cascade, and its kinetic energy. The Z and A numbers are calculated from the charge and baryon number conservation between a target nucleus, a projectile and all secondaries emitted before the evaporation step, and the recoil energy is obtained (see eq. (6) of our previous

paper [4]) assuming the relativistic energy and momentum conservation (even though momentum is conserved only on the average in the FLUKA model) *.

There exists at present clear experimental evidence (see refs. [9,11] and experimental works quoted there) that the intranuclear cascade model developed by Bertini and implemented to the HETC code, which facilitated quite convincing description of this process in the intermediate energy range (100 MeV–5 GeV), fails at higher energies, overpredicting the secondary particle multiplicities when compared to measured data. Another difficulty found by Alsmiller, when trying to couple the FLUKA and HETC models, and again confirmed by our calculations was that the distribution of mass numbers of the residual nuclei obtained by using original EVENTQ + EVAP models showed an unexpected Gaussian shape, whereas curves of measured nuclear production cross sections indicate a peak near the target mass (see, e.g., compilation of Silberberg and Tsao [18]) and the experimental data included in fig. 1). In other words, too many secondaries or/and heavy fragments are emitted, relative to the experimental results, when assuming these models. Thus one could suspect that the E_{inc} or/and E_{ex} sampled in EVENTQ and then provided to EVAP were too high. This means that the formulas for the intranuclear cascade and excitation energies contained in the EVENTQ generator, resulting from a parametrization of the Bertini data, have to be modified.

The necessity of these changes was understood in Alsmillers' work adopting the FLUKA event generator for the new version of HETC code [11]. The main assumption of their modifications in EVENTQ, stimulated by empirical observations, was that the total energy carried by the intranuclear cascade neutrons and protons can be correlated with the number of collisions of the projectile particle with the nucleons of the target nucleus. In addition to the correlation, they had to use phenomenologically determined factors (dependent on the target mass and on the projectile particle, and tabulated in the appendix of their report) for further reduction of the intranuclear cascade energy, to match the measured multiplicities of "gray" particles.

An attempt to explain the above-mentioned discrepancies by a physical picture was made by Ranft [9] who uses the concept of formation time of hadronic states of quark matter after strong interaction to reduce the probability of further collisions of the formed hadrons inside a nucleus, especially at high projectile energies, thus reducing E_{inc} and E_{ex}; implementation of this model into MC shower code is in progress.

* In the previous version of our code the residual atomic mass was also calculated from the four-momentum conservation.

In the current version of FLUNEV code we decided to abandon the old parametrization and to follow exactly Alsmillers' modification of the intranuclear cascade energy, until the formation time value is verified and the new generator is tested and released. Apart from reducing the total energy, the emitted cascade neutrons and protons are sampled from the original FLUKA subroutines, accounting also for the Fermi energy of the nucleus and checking the energy conservation.

Another quantity which seemed to be too high to get consistent results with experimental data was the excitation energy determined in original FLUKA. In the old parametrization of Ranft [21], E_{ex} was assumed to be a function of the projectile energy monotonically increasing up to 3 GeV. Instead of the direct energy dependence, in our version we followed the assumption made in one of the Dubna codes [10] that the excitation energy is also correlated with the number n of collisions of the projectile particle within the struck nucleus, which is equivalent to the number of "wounded" (hit by projectile) nucleons. This parameter is sampled event-by-event by using the NUDIST function of FLUKA which is called in our version immediately after entering the event generator, i.e. still before the decision is made between the two alternative models of EVENTQ, NUCEVT (the parton model, above 5 GeV/c) or NUCRIN (intermediate momentum model). The random fluctuations of the excitation energy are introduced by sampling it from the exponential distribution parametrized by n, proposed by Campi and Hüfner (see ref. [31], eq. (2.3))

$$f(E_{ex}) = \frac{1}{(n-1)!}\,\frac{E_{ex}^{n-1}}{E_0^n}\,\exp\left(-\frac{E_{ex}}{E_0}\right). \tag{1}$$

A certain semi-empirical mean amount E_0 of excitation energy per wounded nucleon (somewhat arbitrary set to 23 MeV in the Dubna report) was assumed by us to be a slowly increasing function of the atomic mass A of the target,

$$E_0 \simeq cA^{1/2}, \tag{2}$$

as it was originally done in the FLUKA parametrization below 100 MeV; the reason for this approximation is that the old Ranft model below 100 MeV had given a reasonable shape of the mass distribution of residual nuclei, and that only one projectile collision inside the target nucleus can be expected on the average at such low energies. The coefficient c was readjusted to 6 MeV providing a better consistency of evaporated neutron yields with HETC/KFA results (see table 2 in section 2.2).

Our new parametrization does not involve determination of E_{ex} directly from energy conservation (like in Alsmiller's work quoted above), however it attempts to avoid discontinuity between the two models (NUCEVT and NUCRIN) and introduces to FLUKA

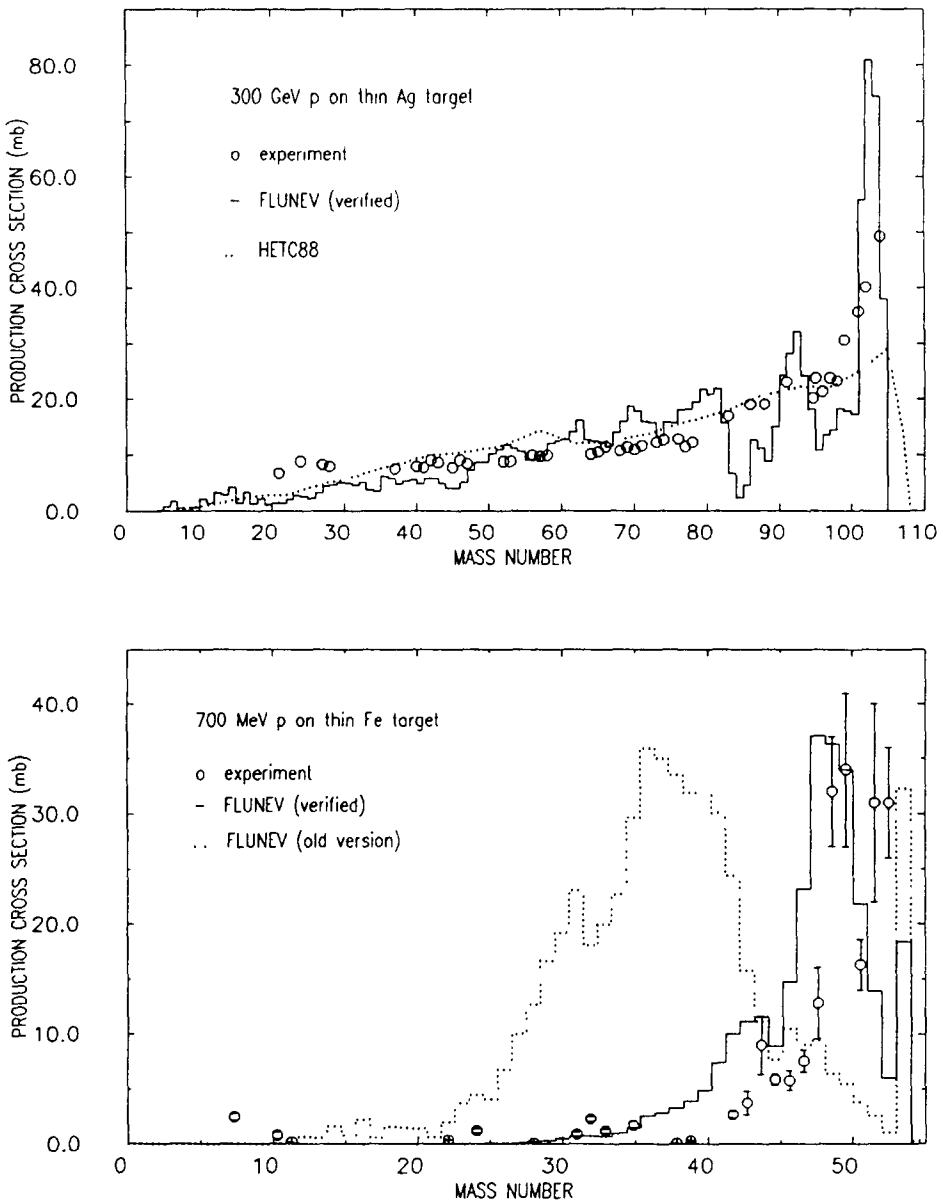

Fig. 1. Mass distributions of residual nuclei for 300 GeV protons incident on a thin Ag target and for 700 MeV protons on an Fe target, as calculated with the FLUNEV code and compared with the new version of the HETC code [11] and with experimental data [18].

the experimentally confirmed prediction that both the energies, carried by the intranuclear cascade and spent for the excitation, are cross-correlated. Note that such determined value of E_{ex} is subject to further modifications in the original NUCRIN until it fulfills the energy conservation requirement. Our possibly simple solution may have temporary character * and it may be improved or replaced in the succeeding version of FLUKA generator prepared at CERN.

The plots in fig. 2 of our paper show the correlations between the projectile energies and the excitation energies determined from the old (upper plot) and the modified (lower plot) model, collected from large samples of all simulated inelastic collisions for a thick iron target irradiated by protons. The excitation energies in the verified version are significantly lower. Furthermore, the discontinuity in the old FLUKA parametrization at the limiting momentum (5 GeV/c) between the

* Anyone interested in the current version of our code and/or in its updated detailed description is requested to contact the authors at DESY.

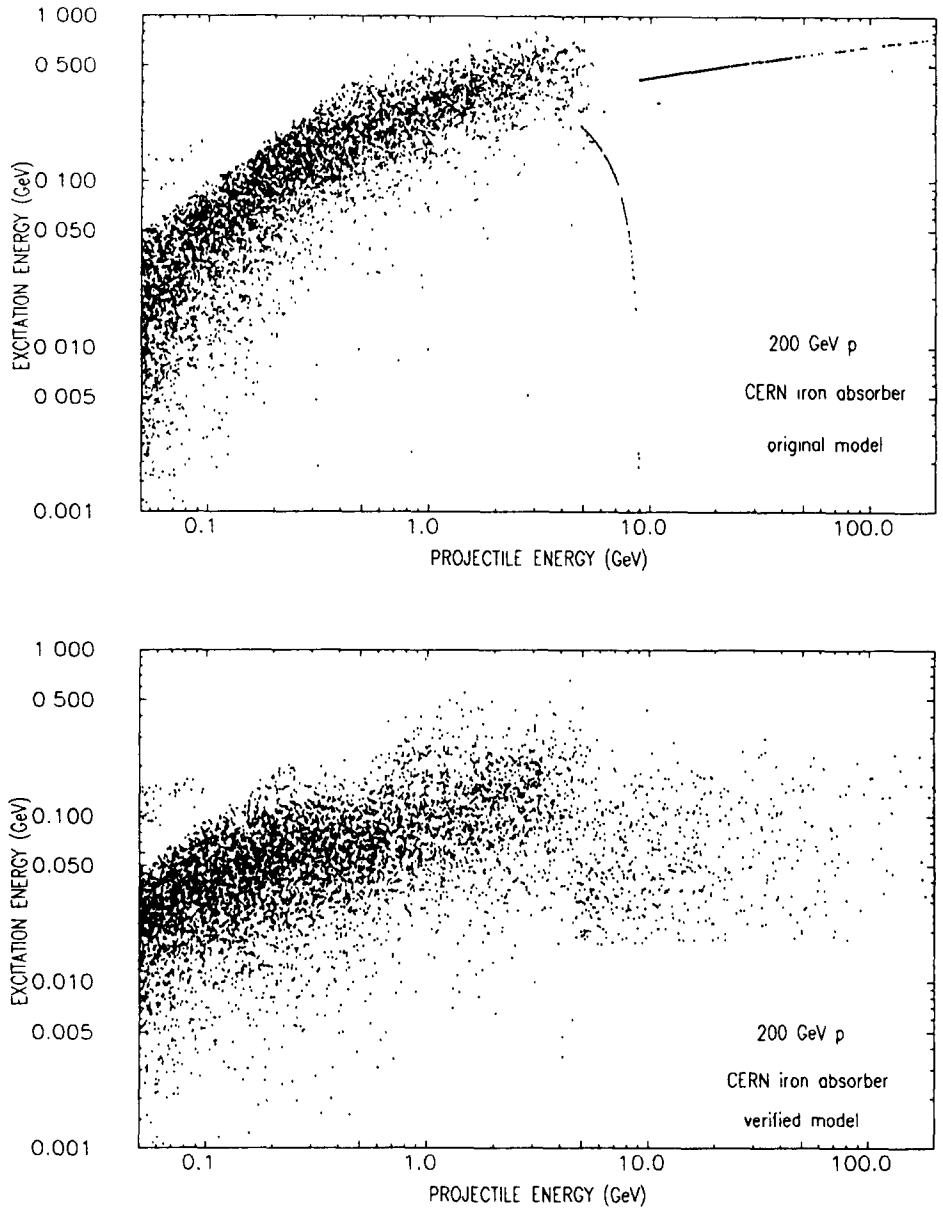

Fig. 2. Excitation energies versus projectile kinetic energies at inelastic interactions in the cascade initiated by protons in iron, as obtained from the old and the corrected model.

parton model (subroutine NUCEVT) and the intermediate energy model (subroutine NUCRIN) is reduced. The mean excitation energies preceding the evaporation process, as they are determined from the old and the modified model are included in table 1. The table contains also excitation and recoil energies of the residual nucleus after evaporation and the resulting yields and mean energies of the evaporation products, averaged over inelastic collisions in a thin iron target irradiated by 590 MeV protons and in a thick iron target irradiated by 200 GeV protons. The large reduction of the excitation energy in the modified version (factor of 3) significantly diminishes the multiplicities and energies of the emitted low energy secondaries.

The lowered E_{inc} and E_{ex} parameters also give much better distributions of the masses of residual nuclei than the original parametrization, as can be seen by comparing the histograms with the experimental points in fig. 1. It shows two examples, one (upper plot) from the high energy range of primary particle (NUCEVT domain) and one (lower plot) from the intermediate incident energy range (NUCRIN domain).

Table 1
Mean input parameters and results of the evaporation model implemented in FLUNEV obtained with the old and the modified version of the code, for protons incident on thin and thick iron targets

	Initial excitation energy	Residual excitation energy	Residual recoil energy	Evaporated neutrons	Evaporated protons	Evaporated heavies
590 MeV p/thin Fe target – original E_{ex}						
Energy [a]						
Yield [b]	205	5.9	2.8	6.2	9.1	12.4
				4.4	3.4	2.4
590 MeV p/thin Fe target – modified E_{ex}						
Energy						
Yield	64	5 9	1.3	3.5	6.5	10.0
				1.9	1 6	0.3
200 GeV p/thick Fe target – original E_{ex}						
Energy						
Yield	156	5.5	3.3	7.2	10.4	14 6
				3 0	2.4	1.8
200 GeV p/thick Fe target – modified E_{ex}						
Energy						
Yield	62	5 8	2.0	4.0	7 3	12.0
				1.7	1.5	0 4

[a] In MeV; for neutrons, protons and heavies per emitted particle, averaged over all inelastic collisions in the system
[b] In particles per inelastic interaction; averaged over al inelastic collisions in the system.

The dotted line in the upper part of fig. 1 (300 GeV protons on thin Ag target) includes Alsmillers' results from the new version of HETC, containing EVENTQ modified by them, giving also an improved mass distribution. Note that all three compared data sets (experimental, FLUNEV and HETC) have been normalized to the same total cross section (obtained by summing the partial cross sections for various produced nuclei), and that our code and HETC still use quite different approaches for evaluating the excitation energies.

2.2. Secondary neutron yields and energy spectra

Determining yields, energy spectra and angular distributions of the secondary neutrons at each inelastic collision is the most important task of the event generator in MC shower code, when applied for estimating neutron fluences to be expected at proton absorbers. For our case of an iron absorber it is important to understand that in thick targets, and particularly at transverse directions, even for very high beam energies

Table 2
Numbers of the cascade neutrons, of the evaporated neutrons and total neutron yields per inelastic collision, for two incident proton energies and thin targets of three elements, calculated with the FLUNEV (the original version and the corrected version) and with the HETC/KFA [15] code

Target element	Process	318 MeV p			800 MeV p		
		FLUNEV original	FLUNEV verified	HETC KFA	FLUNEV original	FLUNEV verified	HETC KFA
C	casc.	0.63	0.60	0.37	1.01	0.99	0.67
	evap.	1.07	0.35	0.09	1.25	0.59	0.17
	total	1.70	0.96	0.46	2.26	1.58	0.84
Al	casc.	0.65	0.64	0.68	1.21	1.19	1.34
	evap.	1.67	0.56	0.33	2.31	0.85	0.71
	total	2.32	1.20	1.02	3.52	2.04	2.05
Pb	casc.	1.06	1.09	1.86	1.99	2.12	4.68
	evap.	9.76	6.64	6.33	16.3	11.5	10.7
	total	10.8	7.73	8.19	18 3	13.6	15.4

the effective projectile energy available for an inelastic interaction is almost immediately reduced below a few GeV, so the secondary neutrons of energies above 1 GeV, although very penetrating, represent only a high energy tail of the whole neutron spectrum and an insignificant fraction of the total neutron fluence in the shower. Therefore, and since we did not introduce any changes into the high energy hadron interaction model of FLUKA, we present and discuss here the calculated neutron production by intermediate energy protons and for secondary neutron energies extended down to 1 MeV, where our modifications have the most important consequences. This is just the well established domain of the standard HETC code, and thus a comparison with HETC results is very useful for the verification of our method. Invariant cross sections for the inclusive production of energetic neutrons by protons of very high energy (400 GeV) on various isotopes have been calculated by the EVENTQ generator elsewhere [12] and compared with available experimental data.

Yields of the cascade neutrons, of the evaporated neutrons and the total neutron yields, for two proton beam energies and thin targets of three elements, are presented in table 2, as obtained from the old and the corrected versions of the FLUNEV code. The determination of total neutron yields from thin targets is a difficult experimental and theoretical task (see e.g. ref. [14]). Therefore the HETC/KFA results [17], given also in table 2, are at present the best reference data available for us. It is apparent that the old FLUNEV model overestimated secondary neutron yields when compared with HETC. The new model matches the reference results at intermediate target masses (^{27}Al; the same can be assumed for ^{56}Fe). For heavy target elements (^{208}Pb) the total yields are in rough agreement, however the cascade neutron yields predicted by FLUNEV are lower than those from HETC and this is partially compensated by somewhat higher yields of evaporated neutrons. Discrepancies occur for light nuclei; one can, however, doubt if the results for ^{12}C are meaningful since the formation of a compound nucleus assumed by the evaporation model (included in FLUNEV and HETC) is not an accurate physical picture accounting for possible processes like prompt fragmentation of a light nucleus.

Secondary neutron spectra for angles of emission around 30°, 90° and 150° relative to a 590 MeV proton beam incident on a thin iron target had been analyzed by Filges et al. [16]. The measured data had been compared with HETC/KFA calculations. This comparison is reproduced in fig. 3 together with the results obtained from the old and the modified versions of FLUNEV. At 30° our old model overpredicted emission in the evaporation energy range, but the corrected model meets quite well the experimental points. For 90° both the FLUNEV and the HETC model significantly underestimate a high energy part of the secondary neutron spectrum above 50 MeV. At 150° the modified FLUNEV model surprisingly gives a high energy neutron production (above 100 MeV) larger than the old model, the HETC/KFA calculations or the measurements, which still has not been understood. We could mention that the quoted experimental spectra are not considered as final results, and new similar experiments were performed recently by KFA/LANL group [17]; unfortunately, no results are available for iron, and measured cross sections for production of secondary neutrons are reported only above 5 MeV.

3. Comparison with thick target experiments and calculations

3.1. Influence of changes in model on thick target results and comparison with earlier data

Estimation of the neutron field around a thick target (beam absorber, calorimeter) involves not only the neutron production model (discussed in the previous sections), but requires also the description of nuclear reactions and of propagation of low energy neutrons. We made a test of this part of calculations by extracting the low energy neutron transport module from the FLUNEV code and running it as a remote program, sampling a purely neutronic source (instead of providing neutrons from high inelastic interactions). The reference system was a solid iron block irradiated by a broad beam of 14 MeV neutrons, which is a benchmark problem analyzed by Hendricks and Carter [19] using the MC neutron transport code MCNP and ENDF/B nuclear data base [28] (versions B-IV and B-V).

Fig. 4 shows a comparison of the neutron fluences, per unit lethargy and per unit fluence incident on the front surface of the absorber, obtained at a depth of 100 cm in iron. The fluence magnitudes from both calculations agree well between a few MeV and 1 eV. The neutron spectrum between 14 MeV and 2 MeV could not be reproduced by the analog FLUNEV simulation, because the unscattered and once-scattered neutrons are the most abundant in that energy range, but at 100 cm depth in iron they contribute less than 10^{-5} of the total fluence; thus scoring of them (accomplished by e.g. MCNP or MORSE) requires application of sophisticated biasing techniques which still have not been used in FLUNEV.

In the example described above the FLUNEV results were obtained from the previous version of our code, using the HILO82 multigroup neutron cross section library (below 20 MeV based on ENDF/B-IV data), with anisotropic scattering approximated by P_3 Legendre expansion. In the current version of FLUNEV the old HILO82 [29] data have been exchanged by the

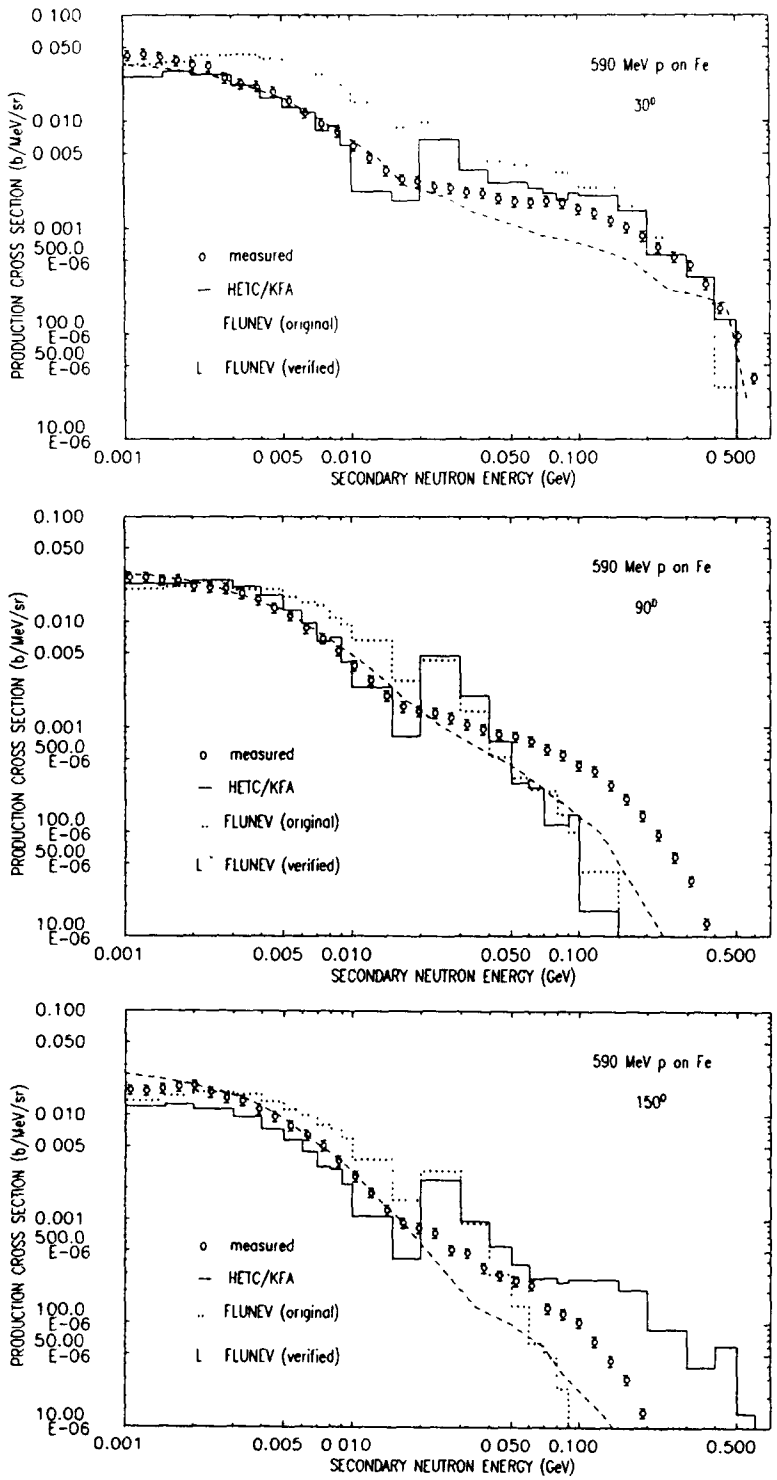

Fig. 3. Energy distributions of secondary neutrons produced at three angles by 590 MeV protons on thin Fe target, calculated with two versions of the FLUNEV code and compared with measured data and distributions obtained by means of the HETC/KFA code (provided by Filges et al. [16]).

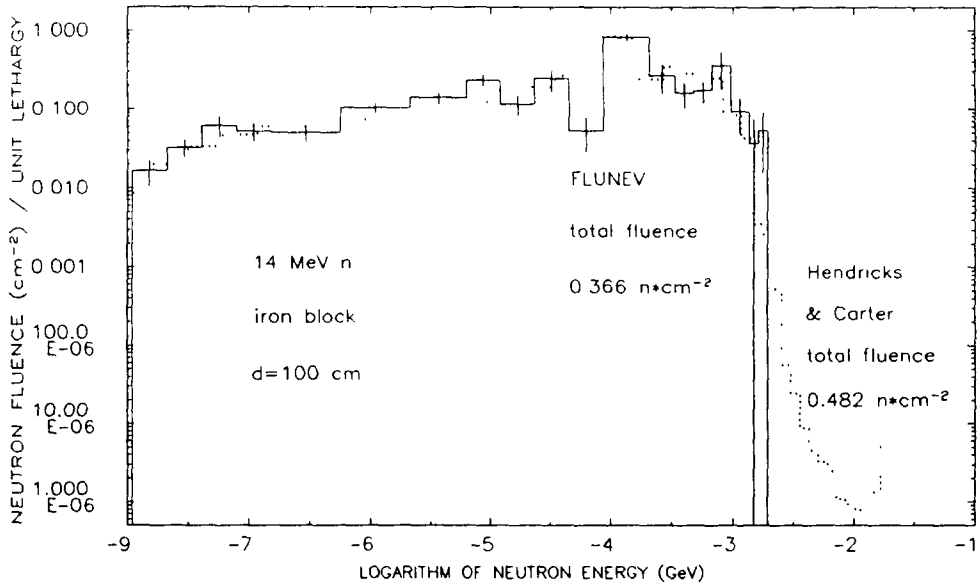

Fig. 4. Comparison of the neutron spectra at 100 cm depth in a solid iron block irradiated by 14 MeV neutrons, calculated with the FLUNEV code and the HILO82 library and by Hendricks and Carter [19] using the MCNP code with ENDF/B-IV data.

HILO86 library [30] with more elements available, with significant corrections above 20 MeV, with the part below 20 MeV based on the ENDF/B-V data and with P_5 Legendre expansion. Differences in the neutron cross sections of iron could result in significant differences of the neutron spectra, but comparison of neutron transport calculations performed by using different nuclear data bases had been done elsewhere [19] and is outside the scope of this work.

At high energies we made a comparison of calculated neutron spectra around an iron beam absorber with the results obtained by Gabriel and Santoro [13] using the HETC code. They calculated the spectra of secondary neutrons emerging from a cylindrical iron block of 200 cm length and 81 cm diameter, irradiated by 200 GeV protons. Their results for the lateral leakage spectrum (upper plot) and for the front surface albedo spectrum (lower plot) are compared in fig. 5 with the histograms obtained from the current version of FLUNEV code (modified production model + HILO86 library; solid histograms on the plots) and from the previous version of FLUNEV (old production model + HILO82 library; dotted lines).

The lateral leakage spectra agree well except for energies below 1 keV where our new results tend to be lower. In the albedo spectra the high energy neutron fluences (above 100 MeV) are considerably reduced in our calculations relative to HETC. This behavior is due to the features of the EVENTQ module at energies above the evaporation and intranuclear cascade energy, which is quite different from the old high energy model of the HETC code from 1972 (based on Feynman scaling). The intermediate and low energy neutron fluences obtained from the new version of FLUNEV have significantly been lowered when compared with the previous version of the same code. One can argue, however, that the discrepancies occurring in the range of the spectra below 50 MeV may be caused partly by the differences between the HILO82 and HILO86 cross section representations.

Numerical results obtained from both versions are given in table 3. It can be seen again that substantial differences between the total neutron fluences obtained from both models appear only for the front albedo ($z = 0$ cm) and for the lateral leakage from the most forward absorber region ($z = 0$–50 cm); for the leakage through the back face and through side surfaces near the end of the absorber the two models of FLUNEV do not differ. This observation leads to the conclusion that for very thick targets, in which a cascade is well developed, the estimated neutron fluences are not too sensitive to our modifications made in the EVENTQ module due to a fast reduction of the projectile energies to about 100 MeV and lower, where old and new models become similar. This is also confirmed by our observation that even the previous model was able to provide quite reasonable mass distributions of residual nuclei for thick targets (see, e.g. the maxima in the residual mass distribution plotted in fig. 3 of our previous paper [4]), although the thin target mass yield curves were evidently wrong (see the previous section). Therefore we could expect that our former results for bulk shielding [4] would not be significantly affected by the recent changes in FLUNEV code described in this report. This

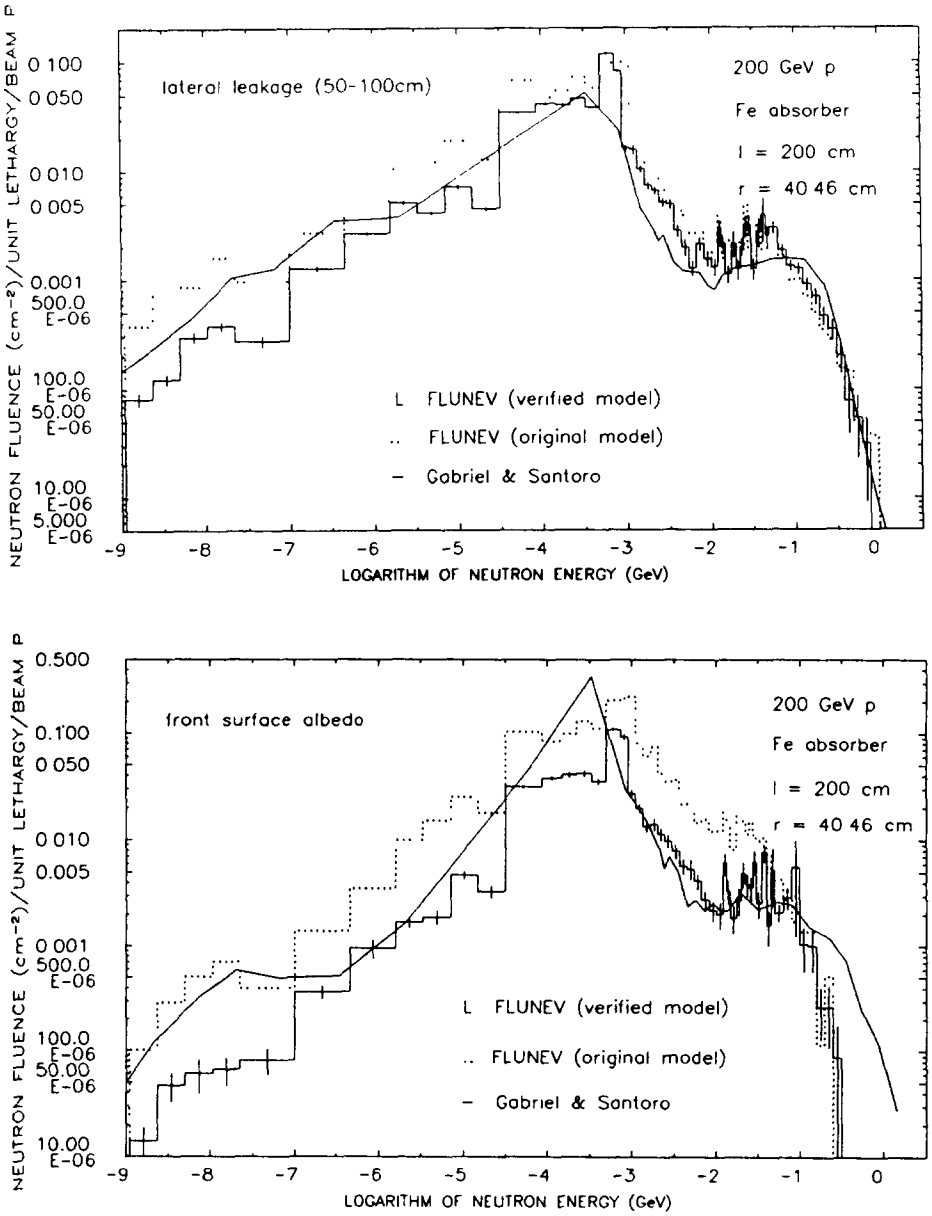

Fig. 5. Comparison of the neutron leakage spectra from the lateral surface and from the front side of an iron absorber irradiated by 200 GeV protons, as calculated by Gabriel and Santoro [13] and with the FLUNEV code.

was confirmed for neutron fluences and dose equivalents outside the lateral shields of ordinary and heavy concrete, obtained from our code with verified model and exchanged cross section library and compared with the data of ref. [4] at 100 GeV.

Table 3 also contains numerical information concerning the neutron spectra, in form of fractions of the total neutron fluences in different energy intervals, at various positions in the absorber. Both models predict the major contributions of more than 90% of the total fluences from the neutrons with energies below 3 MeV. The contribution from the energy range between 0.1 and 3 MeV, dominated by evaporated neutrons, is lowered by the new model. The most drastic reduction due to the modified model is visible for the energy range above 30 MeV, dominated by the most energetic part of evaporation spectrum and by the cascade neutrons.

Another check of our calculational model is the comparison with experiments by means of k_2 values.

Table 3
Comparison of the total neutron fluences and their fractions in different energy intervals, as obtained from the previous and the corrected model of the FLUNEV code, for a thick iron absorber irradiated by 200 GeV protons

	Lateral surface			Transverse boundaries		
z range [cm] [a]	0–50	50–100	100–150	$z = 0$	$z = 100$	$z = 200$
Previous FLUNEV model						
Total fluence [cm^{-2}]	5.69-2 [b]	6.11-2	2.48-2	8.44-2	6 23-1	7.88-3
Relative error	0.05	0.04	0.08	0.08	0 19	0.33
Fraction in energy interval [MeV]						
< 0.1	0.38	0.36	0.37	0.30	0 55	0.28
0.1– 3	0.59	0.60	0.59	0.64	0.42	0.59
3 –10	0.010	0.011	0.012	0.023	0.012	0.034
10 –30	0.007	0.009	0.010	0.020	0.009	0 037
> 30	0.014	0.020	0.020	0.024	0.012	0.062
Modified FLUNEV model						
Total fluence [cm^{-2}]	2.58-2	4.07-2	2.39-2	2 76-2	4 15-1	7.15-3
Relative error	0.04	0.03	0.04	0 06	0 07	0.12
Fraction in energy interval [MeV]						
< 0.1	0 46	0.46	0.46	0.33	0.61	0.34
0.1– 3	0 52	0.52	0.50	0.60	0 37	0.57
3 –10	0.008	0.011	0.012	0.032	0.013	0.031
10 –30	0.008	0.007	0.008	0.023	0.007	0.023
> 30	0.005	0.008	0.012	0.009	0.006	0.037

[a] Proton beam directed along z axis, hits absorber at $z = 0$.
[b] Read as 5.69×10^{-2} (fractional standard deviation below).

The $k_2(E_n)$ factor is defined as the ratio of the neutron fluence $\Phi(E_n)$ [cm^{-2}] above a certain energy threshold E_n [MeV] to the high energy star density S [cm^{-3}] at the same position. Such values had been derived by Tesch and Dinter [1] from some experiments at proton accelerators between 20 and 70 GeV, with S being calculated by means of the fast-running MC code CASIM [22]. The comparison with our results, at different positions along an iron beam absorber of 81 cm diameter is shown in table 4. Note that all star densities have been obtained from CASIM, whereas the calculated neutron fluences are given by the modified version of FLUNEV for the iron absorber and the primary beam energy of the example discussed above. The $k_2(0)$ factors of ref. [1] have been obtained from a rough relationship $k_2(0) \approx 70 k_2(20)$. Though this is a rather crude way of comparison, an agreement within a factor of 2 is satisfying. A more detailed comparison with an experiment performed at high energies is described in the next section.

Table 4
Comparison of k_2 factors near the lateral surface of an iron absorber, as obtained by Tesch and Dinter [1] and from the corrected version of FLUNEV code

	Longitudinal position [cm]			
	0–50	50–100	100–150	150–200
k_2 (20 MeV) [cm]				
Ref. [1]	130	60	8	4
FLUNEV	109	64	23	9
k_2 (0 MeV) [cm]				
Ref. [1]	9100	4200	560	280
FLUNEV	6500	1700	903	240

3.2. Comparison of calculated neutron fluences with CERN iron absorber experiment

Recently Russ et al. [3] have reported measurements of the neutron fluences above 0.1 MeV in a calorimeter-like iron structure irradiated by 200 GeV protons from the CERN SPS. Their research was motivated by lack of experimental information on the number of neutrons produced between 0.1 and 10 MeV from which the highest damage of silicon-based electronics installed at high luminosity colliders is expected. The iron absorber was made of 20 rectangular iron plates of 5 cm thickness. Several kinds of activation detectors and dosemeters were placed in 0.4 cm thick aluminum plates, mounted in 0.7 cm thick slots between the iron layers, and before the first one. Further details concerning the arrangement, types and thresholds of the detectors and the beam profile can be found in the original report.

In our calculations the CERN experimental setup was modeled using the cylindrical geometry package (azimuthal symmetry of the results was confirmed by the experiment) assuming the transverse diameter of the system to be 30 cm and a rectangular beam profile of 1.2×0.9 cm. The energy threshold for neutron trans-

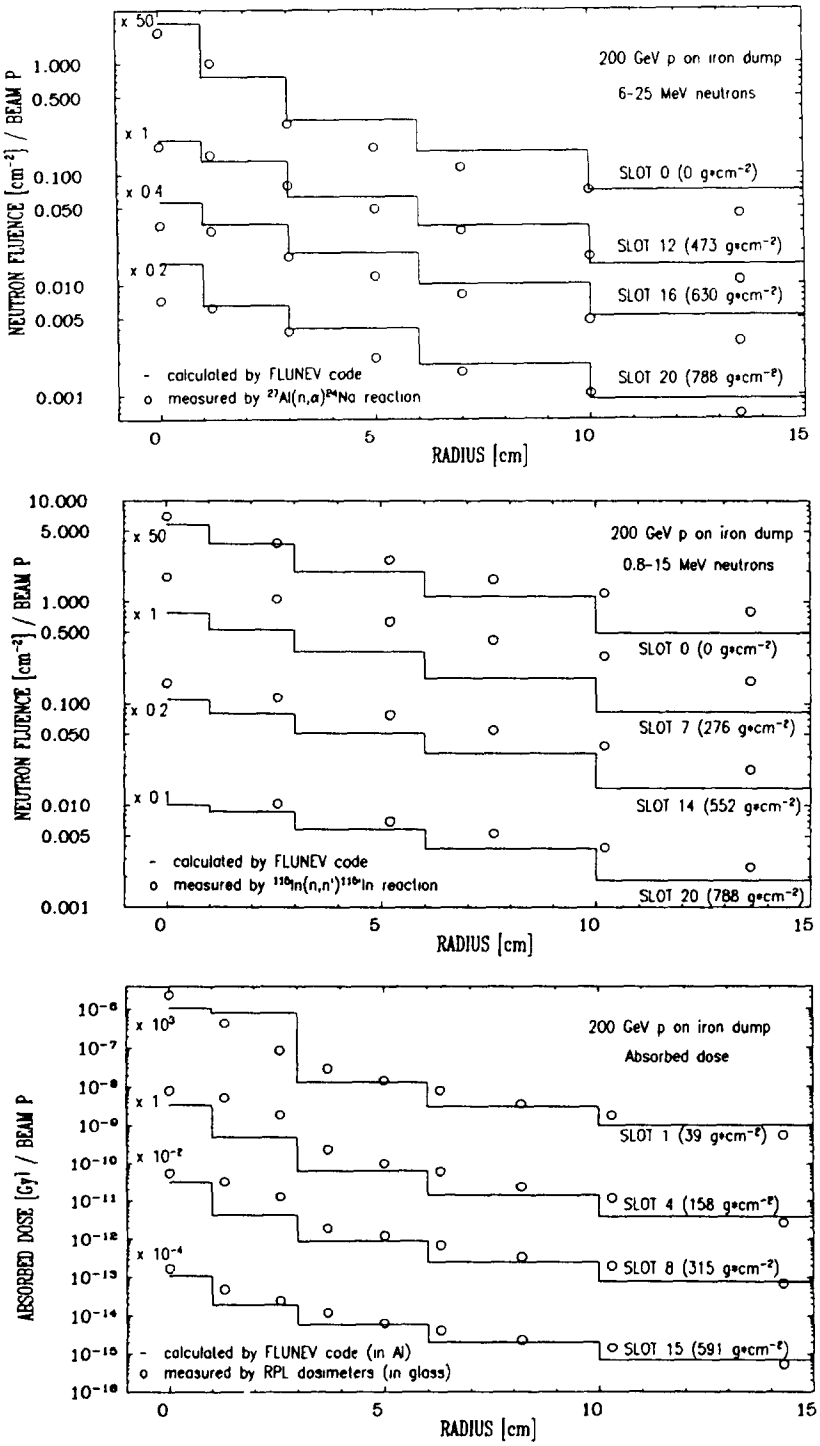

Fig. 6. Comparison of radial distributions of neutron fluences in the energy ranges 0.8–15 MeV and 6–25 MeV and of the absorbed dose, as measured at CERN [2] and calculated with the FLUNEV code.

port in FLUNEV was set to 0.1 MeV. The neutron fluences and the absorbed doses were scored by using the volume tracklength method in 30 geometry regions, corresponding to the aluminum layers from selected six slots divided into five radial ranges. The part of absorbed energy due to the induced electromagnetic cascades was accounted for by using the EGS code coupled to the FLUKA program [32].

To get the final results presented here, two 75 min jobs (differing in a choice of slots for the scoring regions) were run on the IBM-3081 computer, handling on the average 440 beam protons per run and analyzing about 170 inelastic collisions in the whole system per one beam particle. About 3.3 secondary neutrons were emitted per inelastic interaction. This corresponds to an average production of 2.8 neutrons per GeV of incident energy, to be compared with a value of about 3 neutrons per GeV deduced from the measurements [3].

Fig. 6 of our paper presents a comparison of the radial distributions of neutron fluences in the energy ranges 6–25 MeV and 0.8–15 MeV and of the total absorbed doses, as calculated (histograms) with the FLUNEV code (verified model) and as measured (circles) at CERN using various types of detectors. The agreement is good, generally within a factor of 2 or even much better, with some exceptions:

a) for the energy range 6–25 MeV the calculated fluence of albedo neutrons (slot 0) is higher than the measured value;

Table 5
Experimental and calculated ratio of the neutron fluence in energy interval 6–25 MeV to the neutron fluence in energy interval 0.8–15 MeV, versus position in the CERN iron absorber

Radial interval [cm]	Front albedo (slot 0)		Backward leakage (slot 20)	
	FLUNEV	CERN	FLUNEV	CERN
0– 3	0.35	0.34	0.30	0.28
3– 6	0.24	0.18	0.20	0.21
6–10	0.13	0.08	0.17	0.15
10–15	0 14	0.09	0.14	0.14

b) for the energy range 0.8–15 MeV calculations for slot 7 systematically underestimate the experimental data;

c) calculated absorbed doses tend to be systematically lower than measured ones.

We can mention that the fluences given on the plots in the CERN report were derived by using one mean reaction cross section obtained from reference data; accounting for the energy dependence of these cross sections would involve a sophisticated unfolding procedure and it was not done there. A reason of the last discrepancy could be that neither the dose from secondary gamma rays produced in inelastic neutron scattering nor from radiative capture have still been

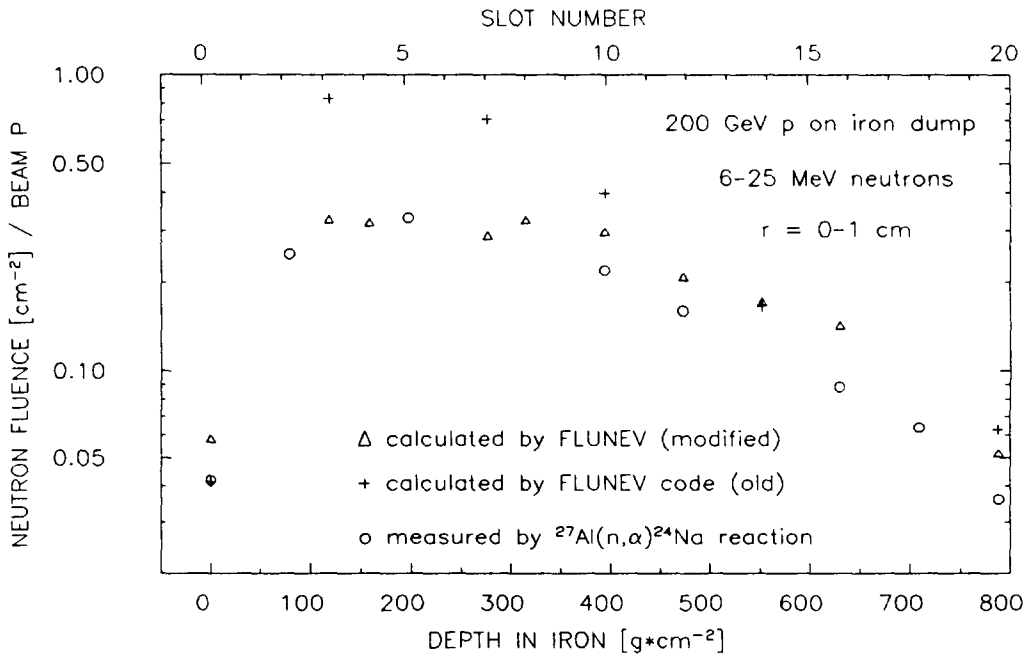

Fig. 7. Comparison of the longitudinal distribution of neutron fluence in the energy range 6–25 MeV, on the beam axis, as measured at CERN [2] and calculated with the FLUNEV code (previous and verified model).

included in the FLUNEV energy deposition model (see ref. [4] for details).

The next figure (fig. 7) presents a comparison of the measured and calculated longitudinal distributions of the neutron fluences between 6 and 25 MeV on the beam axis of the absorber. The calculated results were scored from cylindrical regions of radius 1 cm around the beam axis, the experimental samples had radii between 0.5 and 1.5 cm. Calculation and experiment agree well except for the front face where the fluence of albedo neutrons predicted by FLUNEV is higher than the measured value by almost a factor of two. The results from the previous version of our code are also included, to see the influence of our recent modifications (note that only two versions of the event generator are compared here, but the same cross section library, HILO86, is used). They show much higher fluence values, as expected from the previous sections, except for the fluence of albedo neutrons which surprisingly matches the experimental point.

In addition to comparing the absolute magnitudes of the neutron fluences, it is especially interesting to see if the ratios of the partial fluences measured in different energy ranges are conserved in our calculations. The

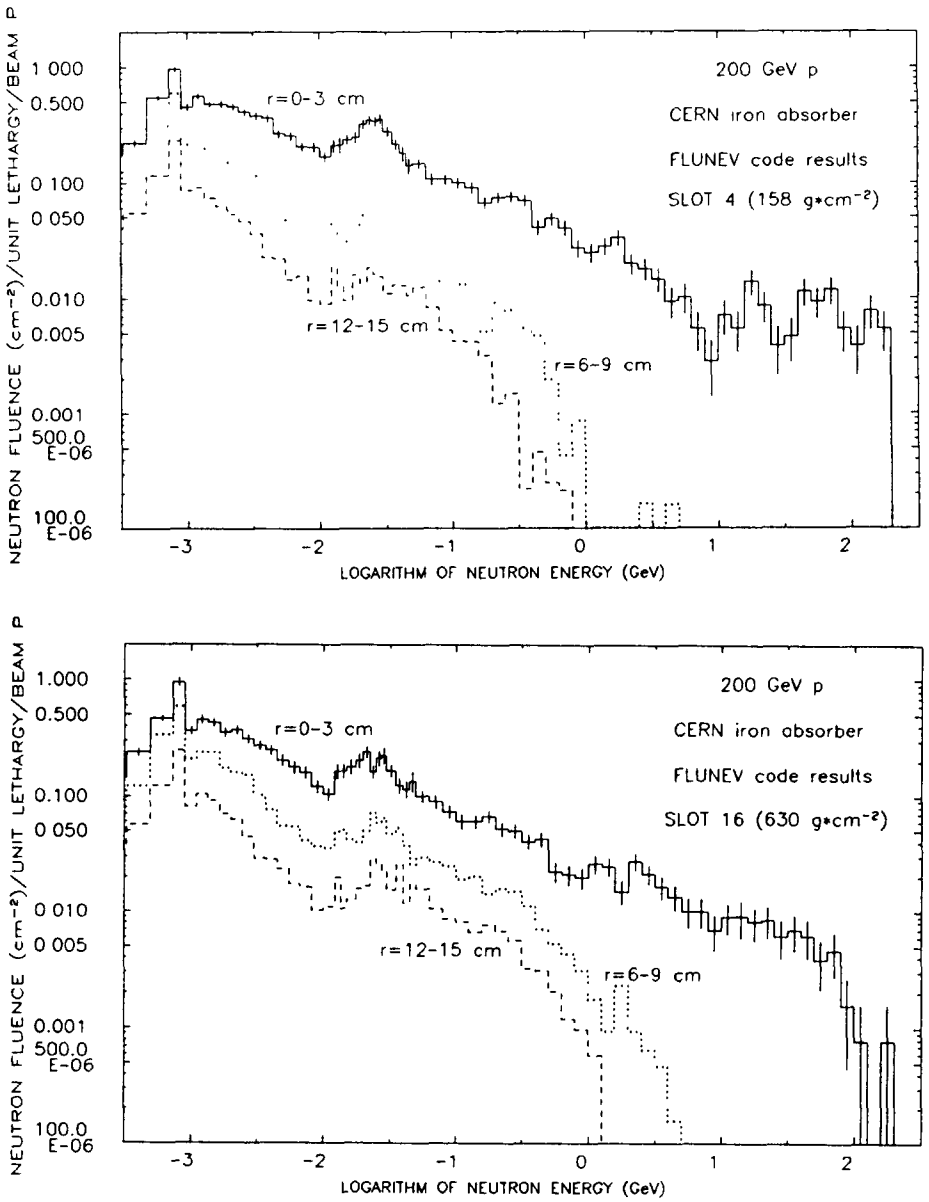

Fig. 8. Neutron fluence spectra calculated with the FLUNEV code for various positions in the CERN iron absorber.

ratios of the fluences between 6 and 25 MeV to the fluences between 0.8 and 15 MeV, obtained from the experimental values and from FLUNEV results, for the front side and for the back side of the absorber, are given in table 5. The agreement is encouraging, and the r dependence of the ratios, showing the hardening of the neutron spectrum in regions near the beam, is well reproduced in our calculations.

The comparison made in table 5 can be considered as an experimental test of the total neutron spectra calculated by FLUNEV, shown in the last fig. 8, for 2 longitudinal and 3 radial positions inside the iron absorber. Tabulated data of the spectra at these and various other positions are available on request from the authors. They can be used for reevaluating the reaction rates of the threshold detectors used in the experiment or for estimating the neutron damage of other instruments.

Acknowledgements

The authors would like to appreciate fruitful discussions and technical aid of many other people: especially thanks are due to H.-J. Möhring from the University of Leipzig for useful explanations of coding details in EVENTQ module; to A. Ferrari from CERN for pointing out some errors in the previous version of FLUKA; to A. Fasso from CERN for describing the experimental setup; to R.G. Alsmiller, Jr. and W.W. Roussin from RSIC/ORNL for providing the HILO86 library; to D. Filges from KFA Jülich for making available the HETC/KFA code and its results; and, finally, to H.-J. Möhring and H. Dinter from DESY for reading the manuscript.

References

[1] K. Tesch and H. Dinter, Radiat. Protection Dosim. 15 (1986) 89.
[2] R.H. Thomas and G.R. Stevenson, IAEA Technical Report Series, no. 283 (Vienna, 1988).
[3] J.S. Russ, G.R. Stevenson, A. Fasso, M.C. Nielsen, C. Furetta, P.G. Rancoita and I. Vismara, CERN Div. rep. TIS-RP/89-02 (1989).
[4] J.M. Zazula and K. Tesch, DESY rep. 89-064 (1989); Nucl. Instr. and Meth. A286 (1990) 279.
[5] H.-J. Möhring, K. Noack and J.M. Zazula, DESY rep. HERA 89-21 (1989).
[6] G.R. Stevenson, CERN Div. rep. TIS-RP/173 (1986).
[7] K. Hänsgen, H.-J. Möhring and J. Ranft, Nucl. Sci. Eng. 88 (1984) 551.
[8] H.-J. Möhring (Leipzig University), private communication;
A. Fasso (CERN), private communication;
D. Filges, KFA Jülich, private communication.
[9] J. Ranft, Z. Phys. C43 (1989) 439.
[10] V.S. Barashenkov, A. Polanski and A.N. Sosnin, Dubna rep. JINR/E2-89-437 (1989), to be published in Acta Phys. Pol.
[11] F.S. Alsmiller and R.G. Alsmiller, Jr., Oak Ridge National Laboratory rep. ORNL/TM-11032 (1985); Nucl. Instr. and Meth. A278 (1989) 713.
[12] R.G. Alsmiller, Jr., F.S. Alsmiller and O.W. Hermann, Oak Ridge National Laboratory rep. ORNL/TM-11257 (1989); Nucl. Instr. and Meth. A286 (1990) 73.
[13] T.A. Gabriel and R.T. Santoro, Oak Ridge National Laboratory rep. ORNL/TM-3945 (1972).
[14] S. Pearlstein, Nucl. Sci. Eng. 95 (1987) 116.
[15] P. Cloth, D. Filges, G. Sterzenbach, T.W. Armstrong and B.L. Colborn, KFA Jülich rep. Jül-Spez-196 (1983).
[16] D. Filges, S. Cierjacks, Y. Hino, T.W. Armstrong and P. Cloth, KFA Jülich rep. Jül-1960 (1984).
[17] P. Cloth, P. Dragovitsh, D. Filges, Ch. Reul, W.B. Amian and M.M. Meier, KFA Jülich rep. Jül-2295 (1989).
[18] R. Silberberg and C.H. Tsao, Naval Research Laboratory rep. NRL-7593 (Washington, 1973).
[19] J.S. Hendricks and L.L. Carter, Nucl. Sci. Eng. 77 (1981) 71.
[20] T.A. Gabriel, Oak Ridge National Laboratory rep. ORNL/TM-9727 (1985).
[21] P.A. Arnio, J. Lindgren, J. Ranft, A. Fasso and G.R. Stevenson, CERN Div. rep. TIS-RP/168 (1986) and TIS-RP/190 (1987)
[22] A. Van Ginneken, Fermi National Accelerator Laboratory rep. FN-272 (1975).
[23] M.B. Emmet, Oak Ridge National Laboratory rep. ORNL-4972 (1975).
[24] M.A. Abdou, C.W. Maynard and R.Q. Wright, Oak Ridge National Laboratory rep. ORNL/TM-3994 (1973).
[25] T.A. Gabriel, J.E. Brau and B.L. Bishop, Oak Ridge National Laboratory rep. ORNL/TM-11060 (1989).
[26] P. Cloth, D. Filges, R.D. Neef, G. Sterzenbach, Ch. Reul, T.W. Armstrong, B.L. Colborn, B. Anders and H. Brückmann, KFA Jülich rep. Jül-2203 (1988).
[27] H. Kowalski, H.-J. Möhring and T. Tymieniecka, DESY rep. 87-170 (1987).
[28] D. Garber, Brookhaven National Laboratory rep. BNL/NCS-17541 (1975).
[29] R.G. Alsmiller, Jr. and J. Barish, Nucl. Sci. Eng. 80 (1982) 448.
[30] R.G. Alsmiller, Jr., J.M. Barnes and J.D. Drischler, Nucl. Instr. and Meth. A249 (1986) 445.
[31] X. Campi and J. Hüfner, Phys. Rev. C24(5) (1981) 2199.
[32] W.R. Nelson, H. Hirayama and D.W.O. Rogers, Stanford Linear Accelerator Center rep. SLAC-225 (1985).